Acknowledgment. We thank Dr. Melvin L. Luetkens, Jr., of the University of Michigan for many helpful suggestions. We thank the NSF for partial support of this work and for funds for the purchase of a FT-NMR spectrometer under Grant CHE76-23334. L.L.L. wishes to thank the Academy of Finland for funds used in support of his visit to the University of Helsinki in July 1984, during which time this paper was completed.

Registry No. Li_4Sn_9, 101419-04-9; Na_4Sn_9, 12533-62-9; K_4Sn_9, 84109-35-3; Rb_4Sn_9, 101419-05-0; Cs_4Sn_9, 101419-06-1; Li_4Sn_8Pb, 101419-07-2; Na_4Sn_8Pb, 101419-08-3; K_4Sn_8Pb, 101419-09-4; Rb_4Sn_8Pb, 101419-10-7; Cs_4Sn_8Pb, 101419-11-8; $Na_4Sn_7Pb_2$, 101419-12-9; $K_4Sn_7Pb_2$, 101419-13-0; $Rb_4Sn_7Pb_2$, 101419-14-1; $Cs_4Sn_7Pb_2$, 101419-15-2; $Na_4Sn_6Pb_3$, 101419-16-3; $K_4Sn_6Pb_3$, 101419-17-4; $Rb_4Sn_6Pb_3$, 101419-18-5; $Cs_4Sn_6Pb_3$, 101419-19-6; $Na_4Sn_5Pb_4$, 101419-20-9; $K_4Sn_5Pb_4$, 101419-21-0; $Rb_4Sn_5Pb_4$, 101419-22-1; $Cs_4Sn_5Pb_4$, 101419-23-2; $Na_4Sn_4Pb_5$, 101419-24-3; $K_4Sn_4Pb_5$, 101419-25-4; $Rb_4Sn_4Pb_5$, 101419-26-5; $Cs_4Sn_4Pb_5$, 101419-27-6; $Na_4Sn_3Pb_6$, 101419-28-7; $K_4Sn_3Pb_6$, 101419-29-8; $Rb_4Sn_3Pb_6$, 101419-30-1; $Cs_4Sn_3Pb_6$, 101419-31-2; $Na_4Sn_2Pb_7$, 101419-32-3; $K_4Sn_2Pb_7$, 101419-33-4; $Rb_4Sn_2Pb_7$, 101419-34-5; $Cs_4Sn_2Pb_7$, 101470-92-2; Na_4SnPb_8, 101419-35-6; K_4SnPb_8, 101419-36-7; Rb_4SnPb_8, 101419-37-8; Cs_4SnPb_8, 101419-38-9; Na_4Sn_8Ge, 101419-39-0; K_4Sn_8Ge, 101419-40-3; Rb_4Sn_8Ge, 101470-93-3; $Na_4Sn_7Ge_2$, 101419-41-4; $K_4Sn_7Ge_2$, 101419-42-5; $Rb_4Sn_7Ge_2$, 101470-94-4; $Na_4Sn_6Ge_3$, 101419-43-6; $K_4Sn_6Ge_3$, 101419-44-7; $Rb_4Sn_6Ge_3$, 101419-45-8; $Na_4Sn_5Ge_4$, 101419-46-9; $K_4Sn_5Ge_4$, 101419-47-0; $Rb_4Sn_5Ge_4$, 101470-95-5; $Na_4Sn_4Ge_5$, 101419-48-1; $K_4Sn_4Ge_5$, 101419-49-2; $Rb_4Sn_4Ge_5$, 101419-50-5; $Na_4Sn_3Ge_6$, 101419-51-6; $K_4Sn_3Ge_6$, 101419-52-7; $Rb_4Sn_3Ge_6$, 101419-53-8; $Na_4Sn_2Ge_7$, 101419-54-9; $K_4Sn_2Ge_7$, 101470-96-6; $Rb_4Sn_2Ge_7$, 101419-55-0; Na_4SnGe_8, 101419-56-1; K_4SnGe_8, 101419-57-2; Na_5Sn_8Tl, 89680-10-4; K_5Sn_8Tl, 101419-58-3; Na_5Sn_7PbTl, 101419-59-4; K_5Sn_7PbTl, 101419-60-7; $Na_5Sn_6Pb_2Tl$, 101419-61-8; $K_5Sn_6Pb_2Tl$, 101419-62-9; $K_5Sn_5Pb_3Tl$, 101419-63-0; $K_5Sn_4Pb_4Tl$, 101419-64-1; $Na_2Sn_2Bi_2$, 101419-65-2; $K_2Sn_2Bi_2$, 82150-33-2; Li_4Pb_9, 101419-66-3; Na_4Pb_9, 101419-67-4; K_4Pb_9, 84109-36-4; Rb_4Pb_9, 101419-68-5; Cs_4Pb_9, 101419-69-6; ^{119}Sn, 14314-35-3; ^{205}Tl, 14280-49-0; ^{207}Pb, 14119-29-0; ^{117}Sn, 13981-59-4; ^{203}Tl, 14280-48-9.

Contribution from the Department of Synthetic Chemistry, Kyoto University, Sakyo-ku Yoshida, Kyoto, 606 Japan

Kinetic Investigation of Uranyl–Uranophile Complexation. 1. Macrocyclic Kinetic Effect and Macrocyclic Protection Effect

Iwao Tabushi* and Atsushi Yoshizawa

Received May 7, 1985

Equilibria and rates of ligand-exchange reactions between uranyl tricarbonate and dithiocarbamates and between uranyl tris(dithiocarbamates) and carbonate were studied under a variety of conditions. The dithiocarbamates used were acyclic diethyldithiocarbamate and macrocyclic tris(dithiocarbamate). The acyclic ligand showed a triphasic (successive three-step) equilibrium with three different equilibrium constants while the macrocyclic ligand showed a clear monophasic (one-step) equilibrium with a much larger stability constant for the dithiocarbamate–uranyl complex. The macrocyclic ligand showed the S_N2-type ligand-exchange rate in the forward as well as reverse process, while the first step of the acyclic ligand-exchange reactions proceeded via the S_N1-type mechanism. This kinetic macrocyclic effect on molecularity is interpreted as the result of a unique topological requirement of uranyl complexation. The macrocyclic ligand also exhibited a clear protection effect, leading to the large stability constant.

Uranyl ion, UO_2^{2+} (U^{VI}), the most stable species among uranium compounds present in nature, has a linear structure[1] with a unique form of ligand coordination. According to X-ray crystallographic studies,[2] usually uranyl complexes have six ligands attached to the uranium center. These ligands are nearly on a plane (with small vertical deviation), which is perpendicular to the UO_2^{2+} ion axis. Anionic ligands are usually favored over neutral ligand complexation, thus leading to the formation of stable anionic coordination complexes. As a consequence, the most stable of all uranium derivatives are hydrophilic and highly soluble in water.

Therefore, most of the uranium on Earth is present in seawater (ca. 10^9 tons) and little is present on the land surface (ca. 10^6 tons).[3] This unusual situation prompted us to design and synthesize "uranophiles"—specific and strong ligands toward uranyl ion—in order to provide a possibility for the efficient extraction of uranyl ions from seawater.[3,5] The extraction experiments have been repeatedly carried out near the Izu Islands with promising results.[6]

Two major mechanisms for the ligand exchange of uranyl complexes—S_N1 type[7] and S_N2 type[8]—have been reported in the literature. However, no detailed discussion has ever been made about what determines the mechanism. In fact, there has been only one rate analysis of the three successive reversible processes in uranyl ligand exchange, and this analysis assumed an S_N2 mechanism without determining the rate order experimentally.[9]

This paper describes the results of detailed studies on the multistep equilibria of the ligand-exchange reactions between carbonate and the dithiocarbamates and on the kinetics of the first step of the forward as well as the reverse reaction. The macrocyclic ligand is first used for comparison with the acyclic ligand, revealing remarkable macrocyclic effects operating in this system. Noteworthy characteristics of the ligand-exchange reaction for the negatively charged macrocycles (uranophiles) are (1) a kinetic *macrocyclic molecularity effect* (the ligand-exchange mechanism is S_N2 type for the macrocycle but S_N1 type for the corresponding acylic ligand) and (2) a macrocyclic protection effect, extremely slow dissociation of macrocyclic uranyl com-

* To whom correspondence should be addressed.

(1) Cattalini, L.; Croatto, U.; Degetto, S.; Tondello, E. *Inorg. Chim, Acta, Rev.* **1971**, *5*, 19.
(2) Zachariasen, W. H.; Pdettinger, H. A. *Acta Crystallogr.* **1959**, *12*, 526.
(3) Tabushi, I.; Kobuke, T.; Yoshizawa, A. *J. Am. Chem. Soc.* **1984**, *106*, 2481.
(4) *Uranium Resources, Production and Demand*; NEA(OECD), Dec 1975. Uranium in land in the readily accessible state is ca. 10^6 tons.
(5) (a) Tabushi, I.; Kobuke, Y.; Nishiya, T. *Nature (London)* **1979**, *280*, 665. (b) Tabushi, I.; Kobuke, Y.; Ando, K.; Kishimoto, M.; Ohara, E. *J. Am. Chem. Soc.* **1980**, *102*, 5947.
(6) Tabushi, I.; Kobuke, Y.; Nakayama, N.; Aoki, T.; Yoshizawa, A. *Ind. & Eng. Chem. Prod. Res. Dev.* **1984**, *23*, 445.
(7) (a) Crea, J.; Diguisto, R.; Lincoln, S. F.; Williams, E. H. *Inorg. Chem.* **1977**, *16*, 2825. (b) Bowen, R. P.; Lincoln, S. F.; Williams, E. H. *Inorg. Chem.* **1976**, *15*, 2126. (c) Geoffrey, J. H.; Stephan, F. L.; Williams, E. H. *J. Chem. Soc., Dalton Trans.* **1979**, 320. (d) Bokolo, K.; Delpuech, J-J.; Rodehuser, L.; Rubini, P. R. *Inorg. Chem.* **1981**, *20*, 992. (e) Ikeda, Y.; Tomiyasu, H.; Fukutomi, H. *Bull. Chem. Soc. Jpn.* **1983**, *56*, 1060. (f) Ikeda, Y.; Tomiyasu, H.; Fukutomi, H. *Inorg. Chem.* **1984**, *23*, 3197.
(8) (a) Hurwitz, P.; Kustin, K. *J. Phys. Chem.* **1967**, *71*, 324. (b) Cattalini, L.; Vigato, P. A.; Vidali, M.; Degetto, S.; Casellato, U. *J. Inorg. Nucl. Chem.* **1975**, *37*, 1721. (c) Edstrom, A.; Johnson, D. A. *J. Inorg. Nucl. Chem.* **1974**, *36*, 2549. (d) Ishii, H.; Odashima, T.; Mogi, H. *Nippon Kagaku Kaishi* **1983**, 1422.
(9) See ref 8a.

0020-1669/86/1325-1541$01.50/0

Table I. Equilibrium (Final) Concentration of Partial Ligand-Exchange Species under Rate Measurement Conditions[a]

total $[CO_3^{2-}]$, 10^{-3} M	$[2^-]$, M	% $UO_2(CO_3)_3^{4-}$	% $UO_2(CO_3)_2 \cdot 2^{3-}$	% $UO_2(CO_3) \cdot 2_2^{2-}$	% $UO_2 \cdot 2_3^-$
5	0.01	86.2[a]	12.9	0.8	
20	0.05	83.0[a]	15.7	1.3	
20	0.10	68.9[a]	26.1	4.5	0.5
20	0.20	48.2	36.5	12.7	2.6

[a] Rate constants are estimated in low-conversion conditions (within ca. 10% conversion); under these conditions, observed rates are mostly concerned with first ligand exchange.

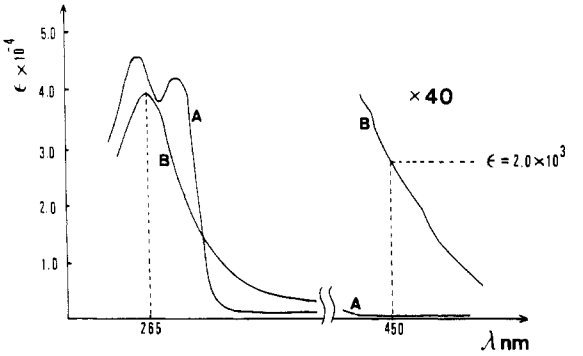

Figure 1. Electronic spectra of **1** and **1**·UO_2 ($[UO_2^{2+}] = 5.0 \times 10^{-6}$ M, $[1] = 7.8 \times 10^{-6}$ M, pH 8.4, $T = 20$ °C): A, **1**; B, **1**·UO_2.

plexes. The latter effect is, of course, a rather general characteristic of macrocyclic ligands known for many other metal ions.[10] Both observed effects seem to have a significant connection with unique *topological requirements* for the coordination between the uranyl ion and the macrocyclic ligand (see below).

Results and Discussion

Triphasic Equilibrium of Uranyl–Diethyldithiocarbamate Complexation and Monophasic Equilibrium of Uranyl–Macrocyclic Tris(dithiocarbamate). Macrocyclic uranophile **1**, prepared from

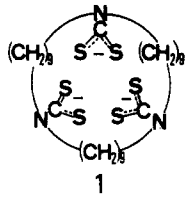

1

2

the corresponding macrocyclic triamine, forms the very stable uranyl complex that shows the characteristic electronic absorption at 265 nm (see Figure 1) with satisfactorily strong absorbance, together with an extended absorption band at longer wavelengths (400–700 nm), where the free dithiocarbamates show no appreciable absorption. This absorption at longer wavelengths is conveniently used for the present equilibrium and rate measurements.[3] Previously, uranyl complexation has not been precisely analyzed in the literature because of the following difficulties: (a) the three (or six) successive steps in coordination proceed with different equilibrium constants and with different rate constants;[11] (b) hydroxide anion attack often competes with the ligand coordination under study, leading to the formation of polynuclear uranyl complexes. In contrast, the present **1**·UO_2^- complex formation is well-defined by a *single equilibrium constant* and by *a pair of rate constants*:

$$1^{3-} + UO_2^{2+}(aq) \underset{k_2}{\overset{k_1}{\rightleftharpoons}} 1 \cdot UO_2^- \qquad (1)$$

$$K = \frac{[1 \cdot UO_2^-]}{[1^{3-}][UO_2^{2+}(aq)]}$$

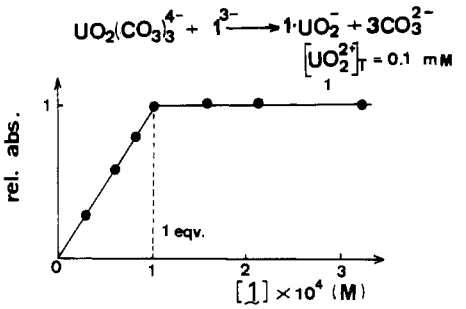

Figure 2. Number of macroligands participating in the complexation with uranyl ion ($[UO_2^{2+}] = 1.0 \times 10^{-4}$ M, pH 9.5, $T = 20$ °C).

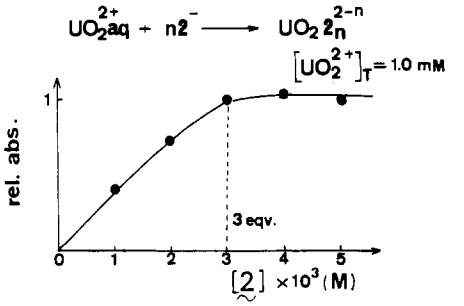

Figure 3. Number of acyclic ligands participating in the complexation with uranyl ion ($[UO_2^{2+}] = 1.0 \times 10^{-3}$ M, pH 5.0, $T = 20$ °C).

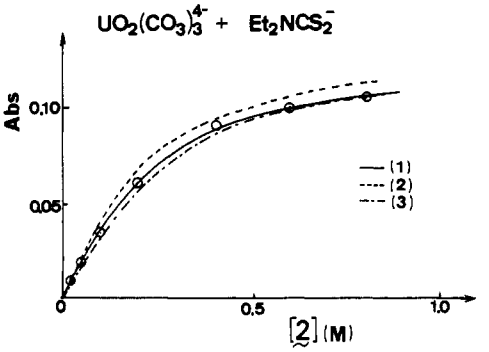

Figure 4. Examples of computer simulation for three successive dithiocarbamate complexations (at 450 nm) showing sensitivity of the curve to small changes in K's ($[UO_2^{2+}] = 1.0 \times 10^{-4}$ M, pH 9.05): (O) experimental value; (1) $K_1 = 8.7 \times 10^{-3}$, $K_2 = 4.0 \times 10^{-3}$, $K_3 = 2.4 \times 10^{-3}$; (2) $K_1 = 8.7 \times 10^{-3}$, $K_2 = 5.0 \times 10^{-3}$, $K_3 = 3.0 \times 10^{-3}$; (3) $K_1 = 7.0 \times 10^{-3}$, $K_2 = 4.0 \times 10^{-3}$, $K_3 = 2.4 \times 10^{-3}$.

This facilitates complexation studies of other ligands L^- via (i) competition kinetics (eq 2a) or (ii) competitive equilibrium (eq

$$1^{3-} + UO_2L_3^- \rightleftharpoons 1 \cdot UO_2^- + 3L^- \qquad (2a)$$

$$1^{3-} + UO_2^{2+}(aq) + 3L^- \rightleftharpoons 1 \cdot UO_2^- \qquad (2b)$$
$$\searrow\!\!\nearrow \; UO_2L_3^-$$

2b). The number of ligand molecules participating in the complexation determined by the absorbance change is 1 for macroligand **1** but 3 for the corresponding monomeric ligand, **2**, as clearly shown in Figures 2 and 3. These results are in excellent agreement with the reported X-ray crystal structure of $2_3UO_2Me_4N$[12] but entirely different from the reported ligand

(10) (a) Tabushi, I.; Fujiyoshi, M. *Tetrahedron Lett.* **1978**, *19*, 2157. (b) Diaddario, L. L.; Zimmer, L. L.; Jones, T. E.; Sokol, L. S. W.; Cruz, R. B.; Yee, E. L.; Ochrymowycz, L. A.; Rorabacher, D. B. *J. Am. Chem. Soc.* **1979**, *101*, 3511.

(11) See ref 8a. There are some reports for other transition metals, e.g.: Hammes, G. G.; Steinfeld, J. I. *J. Am. Chem. Soc.* **1962**, *84*, 4639.

number of 2 or 4 based on spectroscopic measurements.[13] The successive bonding of three molecules of monomeric bidentate ligand, L, to the single UO_2^{2+} ion exhibited a "triphasic" titration curve (i.e., the titration curve characteristic of three competitive, consecutive reactions) as shown in Figure 4. Preliminary estimations of K_1 and K_3 were made under the experimental conditions where (3a) and (3c) are practically the sole contributing equilibria,

$$UO_2L_3 + L' \underset{V_{1'}}{\overset{V_1}{\rightleftharpoons}} UO_2L'L_2 + L \qquad (3a)$$

$$K_1 = \frac{[UO_2L'L_2][L]}{[UO_2L_3][L']}$$

$$UO_2L'L_2 + L' \underset{V_{2'}}{\overset{V_2}{\rightleftharpoons}} UO_2L'_2L \qquad (3b)$$

$$K_2 = \frac{[UO_2L'_2L][L]}{[UO_2L'L_2][L']}$$

$$UO_2L'_2L + L' \underset{V_{3'}}{\overset{V_3}{\rightleftharpoons}} UO_2L'_3 + L \qquad (3c)$$

$$K_3 = \frac{[UO_2L'_3][L]}{[UO_2L'_2L][L']}$$

respectively. Then, the simulation was started in which K_1 and K_3 were changed only in small ranges in order to facilitate the iterative convergence. Computer simulation of the triphasic curve (see Figure 4) gave three different association constants relative to carbonate: $K_1 = 8.7 \times 10^{-3}$, $K_2 = 4.0 \times 10^{-3}$, and $K_3 = 2.4 \times 10^{-3}$ defined by eq 3 where L = CO_3^{2-} and L' = **2**. In an interesting contrast, macrocyclic uranophile **1** showed a clean monophasic (loc. cit.) titration curve, giving a single relative association constant.

The variation of the percentages of the uranyl complexes generated through equilibria 3a–c under the conditions pertaining to the kinetic studies discussed below are shown in Table I.

Triphasic Kinetic Profile for the Monomeric Ligand and Monophasic Kinetic Profile for the Macroligand. Existence of "Kinetic Macrocyclic Effect on Molecularity." Dithiocarbamates **1** and **2** form uranyl complexes that are too stable for dissociation to be observed directly. Therefore, carbonate was chosen as an appropriate counterligand to facilitate the rate and equilibrium measurements of the dithiocarbamate–uranyl complexation via ligand exchange, because of its well-established uranyl complexation and its transparency at 450 nm.

$$UO_2^{2+} + 3CO_3^{2-} \rightleftarrows UO_2(CO_3)_3^{4-} \qquad K = 10^{21.6\pm0.2} \qquad (4)$$

Rate measurements were conveniently done by the use of a stopped-flow system. The reaction proceeds via a successive three-step mechanism, giving the "triphasic" kinetic profile (i.e. three-step competitive consecutive kinetic reaction profile). In an interesting contrast, macrocyclic uranophile **1** gives a clean "monophasic" kinetic profile, demonstrating that the macrocyclic ligand exchange is defined by a pair of rate constants. More interestingly, the kinetic molecularities observed for **1** and **2** are quite different. The observed rate equation of the first (V_{5a}) of the three successive steps for the reaction of monomeric ligand **2** was studied by analysis of the very early stages of the reaction (see eq 5). From the analysis, a typical S_N1-type rate equation

$$UO_2(CO_3)_3^{4-} \underset{CO_3^{2-},\, V'_{5a}}{\overset{2^-,\, V_{5a}}{\rightleftharpoons}} 2\cdot UO_2(CO_3)_2^{3-} \underset{CO_3^{2-},\, V'_{5b}}{\overset{2^-,\, V_{5b}}{\rightleftharpoons}} 2_2UO_2(CO_3)^{2-} \underset{CO_3^{2-},\, V'_{5c}}{\overset{2^-,\, V_{5c}}{\rightleftharpoons}} 2_3UO_2^- \qquad (5)$$

$$V_{5a} = k_{5a}[UO_2(CO_3)_3^{4-}] \qquad (6)$$

(eq 6) is obtained, indicating that the mechanism of the first ligand exchange (V_{5a}) involves rate-determining UO_2^{2+}–CO_3^{2-} bond cleavage (see Scheme I).

Scheme I. Ligand-Exchange Mechanism for Reaction of $UO_2(CO_3)_3^{4-}$ with **2**

$$UO_2(CO_3)_3^{4-} + 2^- \xrightarrow[S_N1 \text{ type cleavage}]{\text{r.d.s.}} O{=}C\overset{O}{\underset{O}{<}}\cdots UO_2(CO_3)_2^{4-} + 2^-$$

$$\longrightarrow UO_2(CO_3)_2^{2-} + 2^- + CO_3^{2-}$$

$$\xrightarrow{\text{fast}} 2\cdot UO_2(CO_3)_2^{3-} + CO_3^{2-}$$

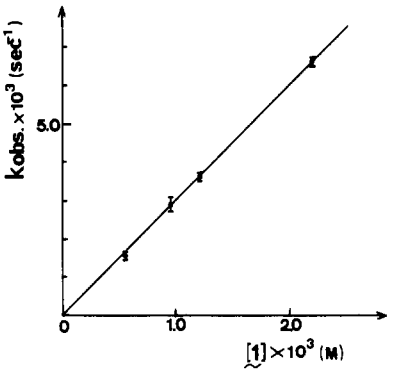

Figure 5. Dependence of observed pseudo-first-order rate constants (k_{obsd}) on **1** concentration for the reaction of $UO_2(CO_3)_3^{4-}$ with **1** ($[UO_2(CO_3)_3^{4-}]$ = 0.1 mM, [1] = 0.5–2.2 mM, T = 20 °C, pH 9.5).

In contrast, the rates of the corresponding ligand exchange of $UO_2(CO_3)_3^{4-}$ with the macrocyclic ligand, **1**, proceed via the second-order kinetics shown in eq 8. This second-order rate

$$UO_2(CO_3)_3^{4-} + 1^{3-} \underset{V'_7}{\overset{V_7}{\rightleftharpoons}} 1\cdot UO_2^- + 3CO_3^{2-} \qquad (7)$$

$$V_7 = k_7[UO_2(CO_3)_3^{4-}][1^{3-}] \qquad (8)$$

equation holds for a variety of conditions (see Figure 5). Therefore, there is a clear distinction between the two ligand exchanges in their kinetic molecularity, which may be called a "kinetic macrocyclic effect on molecularity".

Origin of Kinetic Macrocyclic Effect on Molecularity. Topological Requirement of Macrocyclic Polydentate. Interestingly, it was observed that S_N2 ligand exchange with the macrocyclic ligand, **1**, proceeds much more *slowly* than the corresponding S_N1 reaction with **2** under a wide range of conditions. The isokinetic concentration of **1** estimated from the observed first-order (4.9 s^{-1}; see Figure 10) and second-order (3.0 s^{-1} M^{-1}; see Figure 5) rate constants for **2** and **1**, respectively, is 1.6 M. Below this concentration, the S_N1 route must predominate for **1** unless the S_N1 reactivity of $UO_2(CO_3)_3^{4-}$ is appreciably affected by the slight structural change going from the monomeric to the macrocyclic structure. In fact, however, macrocyclic ligand **1** reacts by the much slower S_N2-type mechanism. Usually, a change in mechanism from S_N1 to S_N2 is explained by the strong nucleophilicity of an entering group perturbing the transition state to convert it to a more stable new S_N2 transition state.[14] In such a case, the S_N2 route is facilitated (in other words, the isokinetic concentration of the entering reagent will be extremely low for good entering groups). The observed high isokinetic concentration suggests the unusual feature of "hindered S_N2". Yet the much faster S_N1-type mechanism does not participate at all.

This unusual result can be explained by the topological requirement (see below) of the macrocyclic polydentate. As schematically shown in Figure 6, the first coordination of a CS_2^- grouping of the macrocyclic ligand to uranyl may proceed similarly to monomeric ligation. However, successive side-on coordination leading to hexacoordination seems topologically unlikely (see

(12) Bowman, K.; Doriz, Z. *Chem. Commun.* **1968**, 636.
(13) Zingaro, R. A. *J. Am. Chem. Soc.* **1956**, *78*, 3568.
(14) (a) See ref 10a. (b) Dishong, D. M.; Diamond, C. J.; Cinoman, M. I.; Gokel, G. W. *J. Am. Chem. Soc.* **1983**, *105*, 586.

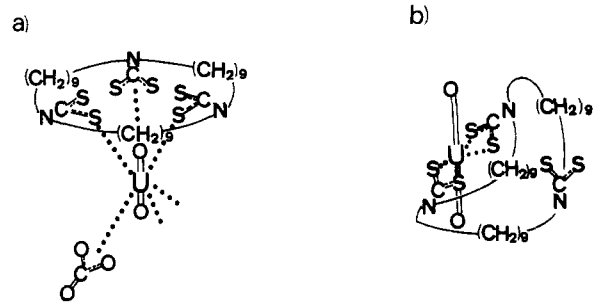

Figure 6. Topologically unfavorable further coordination: (a) edge-on ligand exchange; (b) side-on ligand exchange.

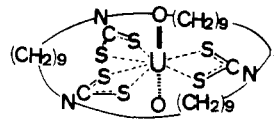

Figure 7. Cavity binding of UO_2 to **1**.

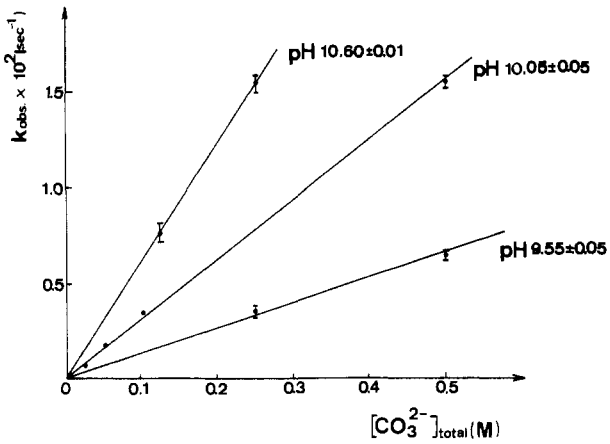

Figure 8. Dependence of observed pseudo-first-order rate constants (k_{obsd}) on total carbonate concentration and pH for the reaction of **1**·UO_2 with carbonate ($[UO_2^{2+}] = (0.9–1.0) \times 10^{-4}$ M, $[\mathbf{1}^{3-}] = (1.3–1.5) \times 10^{-4}$ M, $T = 20$ °C).

Figure 6b). Instead, apical approach seems to lead to the highly stable hexacoordination complex—which is stabilized by the *thermodynamic macrocyclic effect* (see Figure 7).

The first (and/or the second) S_N1-type exchange at the ligand concentration of 0.5–2.2 mM is fast but nonproductive, judging from the equilibrium constants (complex formation amounts less than 1.6% of **2**·$UO_2(CO_3)_2^{3-}$ and 6×10^{-5}% of $\mathbf{2}_3UO_2^-$ at 2.2 mM ligand concentration), while the S_N2-type exchange proceeds productively under these conditions.[15] However, the apical approach must be slow since the approach may suffer from serious steric hindrance (see Figure 6a).

Fast Carbonate Attack on Uranyl Dithiocarbamate Complexes. S_N1-Type and S_N2-Type Routes. Macrocyclic Protection Effect. Dithiocarbamate–uranyl complexes **1**·UO_2^- and $\mathbf{2}_3UO_2^-$ are smoothly converted to $UO_2(CO_3)_3^{4-}$ in a HCO_3^-/CO_3^{2-} buffer. The rates of the ligand exchange were followed at different pH values and different total carbonate concentration, $[HCO_3^-] + [CO_3^{2-}]$ (see Figure 8). At constant pH and constant total carbonate concentration, the ligand exchange of $\mathbf{2}_3UO_2^-$ with carbonate proceeds via a successive three-step mechanism; the first step (V'_{5c}) was studied carefully by following the very early stages of the reaction with a stopped-flow electronic spectrophotometer. Again, a first-order rate equation is observed as shown in eq 9, demonstrating that the reaction proceeds via an

$$V'_{5c} = k'_{5c}[\mathbf{2}_3UO_2^-] \quad (9)$$

S_N1-type mechanism involving U–S bond cleavage in the rate-determining step. However, the rates of the ligand-exchange reaction of **1**·UO_2^- with carbonate increase linearly with increase of total carbonate concentration at constant pH and also increase with pH at constant total carbonate concentration (see Figure 8). The excellent linear correlation between net CO_3^{2-} concentration and observed reaction rate (see Figure 9) demonstrates that CO_3^{2-} is the active attacking species and that the reaction proceeds via an S_N2-type route (eq 10). From the observed pseudo-first-order

$$V'_7 = k'_7[\mathbf{1}\cdot UO_2^-][CO_3^{2-}] \quad (10)$$

rates the second-order rate equation (10) is obtained for the **1**·UO_2^- complex, indicating that the rate-determining cleavage of a U–S bond of **1**·UO_2^- complexes proceeds by the assistance of the entering carbonate. Therefore, the "macrocyclic kinetic molecularity effect" is again clearly demonstrated for the ligand exchange of uranyl dithiocarbamate complexes. As shown in Figure 9, the *second-order rates* are dependent on neither pH nor HCO_3^- concentration, clearly demonstrating that both of the competitive ligand exchanges with OH^- and HCO_3^- are negligible in magnitude compared to the main reaction with CO_3^{2-}. This finding sharply contrasts with the previous observation[16] that OH^- attack led to significant competitive formation of polynuclear uranyl oxide complexes. This remarkable retardation of OH^- attack toward the uranyl ion by the macrocyclic uranophile may be called a "*macrocyclic protection effect*" of a specific ligand for a certain metal ion against degradative hydrolysis in a certain environment. The very slow S_N2-type mechanism for the reaction between **1**·UO_2^- and carbonate can also be explained by the macrocyclic protection effect, as this protection decelerates the otherwise fast S_N1-type U–S cleavage by a factor of at least 55 compared to the case of monomeric ligand **2**.

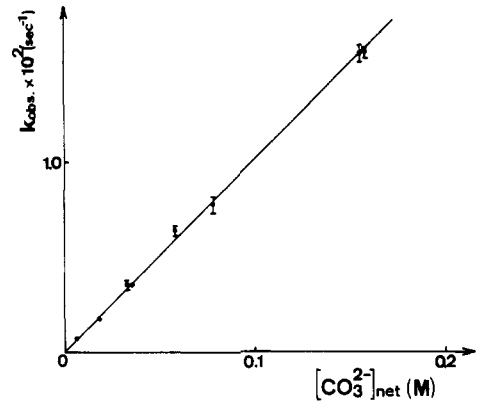

Figure 9. Dependence of observed pseudo-first-order rate constants (k_{obsd}) on net CO_3^{2-} concentration for the reaction of **1**·UO_2 with $[CO_3^{2-}]_{net}$ ($[\mathbf{1}^{3-}] = (1.3–1.5) \times 10^{-4}$ M, $T = 20$ °C).

Experimental Section

Materials. Commercially available uranyl nitrate hexahydrate (Merck reagent grade) was used. Sodium diethyldithiocarbamate purchased from Nakarai Chemical Ltd. (SP) was recrystallized from distilled water (mp 90–91 °C).[17] Trisodium 1,11,21-triazacyclotricosanetricarbodithioate (**1**) was prepared as reported by us previously.[3] IR: 960 cm^{-1}. 60-MHz ^1H NMR: (D_2O, hexamethyldisilazane as external standard) δ 4.1–4.5 (m, 12 H), 1.6–2.4 (m, 2 H), 1.6–1.9 (m, 30 H); (D_2O, disodium 3-(trimethylsilyl)propionate as internal standard) δ 3.8–4.3 (m, 12 H), 1.6–2.1 (m, 12 H) 1.3–1.6 (m, 30 H). 20-MHz ^{13}C NMR: (D_2O, dioxane as an internal standard) δ 112.97 ($N^{13}CS_2$), −12.01 ($N^{13}C$), −38.1 (NC ^{13}C), −39 to −41.2 (other ^{13}C).

General Procedure for Rate Measurements. The ligand-exchange rates under a variety of conditions were followed by observing the electronic spectrum change at 450 nm (see Results and Discussion) with a Union RA-1300 stopped-flow rapid-reaction analyzer or a Union SM 401

(15) A detailed discussion will be described in a forthcoming article.

(16) (a) Ahrlen, D. S.; Hietanen, S.; Sillen, L. G. *Acta Chem. Scand.* **1954**, *8*, 1907. (b) Gustafson, R. L.; Richard, C.; Martell, A. E. *J. Am. Chem. Soc.* **1960**, *82*, 1526.
(17) (a) Mp 92–102 °C: Koch, H. P. *J. Chem. Soc.* **1949**, 401. (b) Mp 92–95 °C: Uhlin, A.; Åkerstrom, S. *Acta Chem. Scand.* **1971**, *25*, 393.

Table II. Molecularity Confirmation for the First and Third Equilibrium Processes (n = 1 Being the Most Satisfactory)[a]

	$\bar{K}_1/[CO_3^{2-}]^n$		
[2], M	n = 0	n = 1	n = 2
0[b]		2.1[c]	
0.005	0.012	2.34	468
0.020	0.062	3.07	153
0.050	0.161	3.22	64
0.100	0.292	2.91	29
	$\bar{K}_3/[CO_3^{2-}]^n$		
[2], M	n = 0	n = 1	n = 2
0.20	3.3	16.5	82.5
0.30	5.1	17.1	57.0
0.40	7.8	19.4	48.5

[a] For $\bar{K}_1$: $[UO_2^{2+}] = 2.0 \times 10^{-4}$ M; $[CO_3]_T = 1.0 \times 10^{-2}$ M; $[CO_3^{2-}]$, $[CO_3^{2-}]_0$, and $\bar{K}_1/[CO_3^{2-}]$ values are calculated on the basis that $[\mathbf{2}_{coord}]/([\mathbf{2}_{free}^-]^n[UO_2(CO_3)_3^{4-}]) = \bar{K}_1/[CO_3^{2-}]$. For $\bar{K}_3$: $[UO_2^{2+}] = 5 \times 10^{-5}$ M; $[CO_3]_T = 5 \times 10^{-3}$ M; $\bar{K}_3/[CO_3^{2-}]$ are calculated on the basis that $[\mathbf{2}_3UO_2^-]/([\mathbf{2}_{free}^-]^n[\mathbf{2}_2UO_2CO_3^{2-}])$ v $\bar{K}_3/[CO_3^{2-}]$; from the listed values, K_3 was estimated to be 2.3×10^{-3}. [b] Extrapolated value to zero concentration from the plot of [2] vs. $\bar{K}_1$. [c] From the first value, $K_1 = 8.9 \times 10^{-3}$.

spectrophotometer equipped with a thermostated cell. All of the measurements were carried out in a sodium bicarbonate/carbonate buffer at 20 °C.

Stopped-Flow Mixing. (A) The ligand-exchange rates of the reaction of uranyl tricarbonate with sodium diethyldithiocarbamate or other exchange reactions were followed spectrophotometrically with a stopped-flow electronic spectrophotometer by rapid mixing of an aqueous solution of uranyl tricarbonate and an aqueous solution of sodium diethyldithiocarbamate in carbonate buffer at pH 9.5. Absorbance at t_0 (time zero) was checked by rapid mixing of carbonate buffer solution (not containing any uranyl ion) and an aqueous sodium diethyldithiocarbamate solution. The background absorbance of $UO_2(CO_3)_3^{4-}$ (0.5–1.0 × 10^{-4} M) at 450 nm was independently ascertained to be negligible. Absorbance of $UO_2(Et_2NCS_2)_3^-$ was measured by rapid mixing of distilled water and a $UO_2(Et_2NCS_2)_3^-$ solution at pH 9.5.

(B) The ligand-exchange rates of the $\mathbf{1}\cdot UO_2^-$ complex with CO_3^{2-} was followed with a Union RT-1300 stopped-flow rapid-reaction analyzer and a Union SM401 spectrophotometer at pH 10.1. Thus, 2.7 mL of an aqueous solution of the $\mathbf{1}\cdot UO_2^-$ complex was mixed with 0.3 mL of an aqueous CO_3^{2-} solution by use of a specially designed syringe that has small holes and a closed tip at the end.[18]

Preparation of a Solution for Stopped-Flow Mixing. A pH 9.5 carbonate buffer solution was prepared by dissolving a 4.0:1.0 molar ratio of sodium bicarbonate to sodium carbonate, respectively, in distilled water. An aqueous uranyl nitrate solution (1.0 mM) was prepared by dissolving 10 mg of uranyl nitrate hexahydrate into 20 mL of distilled water. The uranyl nitrate solution was added to a 40 mM carbonate buffer solution (pH 9.5) to prepare a uranyl tricarbonate solution of an appropriate concentration (0.2–0.4 mM). A solution containing 0.2 mM uranyl nitrate in 20 mM carbonate buffer (pH 9.5) was used for typical rate measurements. An aqueous solution of sodium diethyldithiocarbamate and an aqueous solution of **1** were prepared by dissolving a weighed amount of the carbamate into 20 mM carbonate buffer solution (pH 9.5). The concentration of **1** was determined spectroscopically by measuring the absorbance of the characteristic 283-nm ($\epsilon = 4.1 \times 10^4$) band. An aqueous solution of $UO_2(Et_2NCS_2)_3^-$ was prepared by dissolving sodium diethyldithiocarbamate into aqueous uranyl nitrate; the pH was adjusted to 9.5 with a sodium hydroxide solution.

Estimation of Rate Constants. (A) Ligand-Exchange Rates of Uranyl Tricarbonate with Sodium Diethyldithiocarbamate. Initial concentrations of $UO_2(CO_3)_3^{4-}$ and Et_2NCS_2Na used for the rate measurements ranged between 0.05 and 0.10 mM and between 10 and 200 mM, respectively. The total ligand-exchange process consists of the three steps shown in eq 3. The experimental conditions for the separate rate studies of these three individual steps were optimized on the basis of the equilibrium studies described above. The experimental conditions for the analysis of the first ligand-exchange rate process are shown in Table II, where the reverse reaction V_{-1} was negligible compared with the forward reaction V_1, especially in the early stages of the reaction. V_2 is also negligible in the early stages of the reaction. The rates of the first ligand exchange under

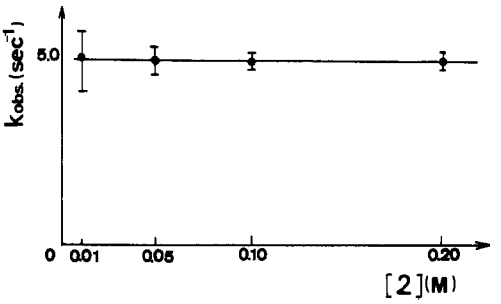

Figure 10. Dependence of observed pseudo-first-order rate constants (k_{obsd}) on [2] for the reaction of $UO_2(CO_3)_3^{4-}$ with **2** ($[UO_2(CO_3)_3^{4-}]$ = 0.1 mM, [2] = 0.01–0.20 mM, T = 20 °C, pH 9.5).

a variety of conditions were conveniently analyzed by simple pseudo-first-order kinetics, as shown in eq 11. The pseudo-first-order rate

$$V = \frac{-d[U_2(CO_3)_3^{4-}]}{dt} = k_{obsd}[UO_2(CO_3)_3^{4-}]$$
$$V_1 = \frac{d[UO_2(CO_3)_2(Et_2NCS_2)^{3-}]}{dt} \qquad k_{obsd} = k_1[Et_2NCS_2^-]^m \tag{11}$$

constants thus obtained for a series of initial concentrations of Et_2NCS_2Na were then plotted against the initial concentrations of Et_2NCS_2Na (see Figure 10). A plot of k_{obsd} vs. $[Et_2NCS_2Na]$ gave a straight line with a slope of m = zero. The intercept thus obtained gave the value of k_1 directly. The kinetic order with respect to $UO_2(CO_2)_3^{4-}$ was also examined by analyzing k_{obsd} values obtained for a series of different intial concentrations of $UO_2(CO_3)_3^{4-}$.

(B) Ligand-Exchange Rates of $UO_2(Et_2NCS_2)_3^-$ with CO_3^{2-}. Initial concentrations of $UO_2(Et_2NCS_2)_3^-$ and total carbonate (HCO_3^- plus CO_3^{2-}) used for the rate measurements were in the ranges 0.05–0.20 and 10–200 mM, respectively. Under these conditions, the rates were analyzed by use of the simple pseudo-first-order equation, as shown in eq 12.

$$V_{-3} = \frac{-d[UO_2(Et_2NCS_2)_3^-]}{dt} = k_{obsd}[UO_2(Et_2NCS_2)_3^-]$$
$$k_{obsd} = k_2[CO_3^{2-}]^n \tag{12}$$

Values of k and n were obtained by the procedure similar to that in (A). The observed value of n is zero, and k_2 is obtained as the observed intercept.

(C) Ligand-Exchange Rates of $UO_2(CO_3)_3^{4-}$ with Macrocyclic Ligand 1. An aqueous solution of uranyl tricarbonate was mixed with an aqueous solution of $\mathbf{1}\cdot 3Na$ in a thermostated water bath at 20 °C and pH 11.3. For the preparation of uranyl tricarbonate, the following conditions were adopted: initial concentrations of uranyl nitrate, sodium carbonate, and $\mathbf{1}\cdot 3Na$ were in the ranges 0.10–0.40, 30–50, and 0.16–0.41 mM, respectively. The electronic spectrum change was observed with a Union SM 401 spectrophotometer equipped with a thermostated cell at 20 °C. Several wavelengths between 440 and 480 nm were selected for the estimation of a relative formation constant of $UO_2\cdot\mathbf{1}^-$. Since the estimated formation constants were nearly equal at different wavelengths, absorbance at 450 nm was mainly used throughout the measurements.

The reverse substitution was also studied. Thus, aqueous $UO_2\cdot\mathbf{1}$ was mixed with aqueous sodium carbonate in a thermostated water bath at 20 °C and pH 11.3. Initial concentrations of uranyl nitrate, sodium carbonate, and $\mathbf{1}\cdot 3Na$ were 0.09, 40, and 0.14 mM, respectively. On the basis of the rate measurements, pseudo-first-order constants were determined for both forward and reverse substitution.

$$V = \frac{-d[UO_2(CO_3)_3^{4-}]}{dt} = \frac{d[UO_2\cdot\mathbf{1}^-]}{dt} = k_{obsd}[UO_2(CO_3)_3^{4-}]$$
$$k_{obsd} = k_3[\mathbf{1}^{3-}]^p \tag{13}$$

From the plot of the observed pseudo-first-order rate constants vs. the initial concentration of $\mathbf{1}^{3-}$, p was determined to be unity (second-order rate) and the value of k_3 was determined from the observed slope.

(D) Rates of Ligand Exchange of $UO_2\cdot\mathbf{1}^-$ with CO_3^{2-}. Initial concentrations of $UO_2\cdot\mathbf{1}^-$ and total carbonate (HCO_3^- plus CO_3^{2-}) used for the rate measurements ranged from 0.09 to 0.2 mM and from 25 to 500 mM, respectively. Measurements were made at pH 9.55, 10.05, and 10.60. Similarly, q in eq 14 was determined as unity and k_4 was obtained from the observed slope.

$$V = \frac{-d[UO_2\cdot\mathbf{1}^-]}{dt} = k_{obsd}[UO_2\cdot\mathbf{1}^-] \qquad k_{obsd} = k_4[CO_3^{2-}]^q \tag{14}$$

(18) Tabushi, I.; Nishiya, T.; Yagi, T.; Inokuchi, H. *J. Am. Chem. Soc.* **1981**, *103*, 6963.

Procedure of Equilibrium Measurements. Number of Ligand Molecules Participating in Complexation with Macrocyclic Ligand 1 or Monomeric Ligand 2. Aqueous uranyl tricarbonate (0.2 mM) was mixed with aqueous **1**·3Na (0.6–6.4 mM) with a carbonate buffer at pH 9.5. The absorbance of UO_2·**1**$^-$ at 450 nm was measured with a Union SM 401 spectrophotometer. Aqueous uranyl nitrate (2.0 mM) was mixed with aqueous sodium diethyldithiocarbamate (2.0–10.0 mM) for the measurement of the UO_2·**2** formation equilibrium.

Equilibrium Measurements. A quantity of 0.1 mM aqueous uranyl tricarbonate was mixed with aqueous sodium diethyldithiocarbamate in 20 mM carbonate buffer, pH 9.05. The initial concentration of sodium diethyldithiocarbamate ranged from 25 to 800 mM. The absorbance change at 450 and 480 nm was measured with a Union SM 401 spectrophotometer. Molar orders with respect to **2** for the first and third equilibrium steps are independently ascertained, as shown in Table I.

Estimation of Equilibrium Constants. Estimation of equilibrium constants were carried out on an NEC PC-8801 personal computer. In the course of the ligand-exchange reaction of $UO_2(CO_3)_3^{4-}$ with **2**, four different coordination states, $UO_2(CO_3)_3^{4-}$, $UO_2(CO_3)_2$·$\mathbf{2}^{3-}$, $UO_2(CO_3)$·$\mathbf{2}_2^{2-}$, and UO_2·$\mathbf{2}_3^-$, should be present as shown in eq 10. Under the present experimental conditions, the absorbance is expressed by eq 15 where the following assumptions are made:[19] $\epsilon_1 = \epsilon_0$, $\epsilon_2 = 2\epsilon_0$, $\epsilon_3 = 3\epsilon_0$.

$$\text{abs} = \epsilon_1[UO_2(CO_3)_2\cdot\mathbf{2}^{3-}] + \epsilon_2[UO_2(CO_3)\cdot\mathbf{2}_2^{2-}] + \epsilon_3[UO_2\cdot\mathbf{2}_3^-]$$

$$K_1 = \frac{[UO_2(CO_3)_2\cdot\mathbf{2}^{3-}][CO_3^{2-}]}{[UO_2(CO_3)_3^{4-}][\mathbf{2}^-]}$$

$$K_2 = \frac{[UO_2(CO_3)\cdot\mathbf{2}_2^{2-}][CO_3^{2-}]^2}{[UO_2(CO_3)_2\cdot\mathbf{2}^{3-}][\mathbf{2}^-]^2} \qquad K_3 = \frac{[UO_2\cdot\mathbf{2}_3^-][CO_3^{2-}]^3}{[UO_2\cdot(CO_3)\mathbf{2}_2^{2-}][\mathbf{2}^-]^3} \tag{15}$$

The absorbance is also expressed by eq 16 by using the equilibrium relationship. The initial (before iterating) values of K_1 and K_3 were

$$\text{abs} = \frac{[UO_2^{2+}]_T\epsilon_0 K_1\dfrac{[\mathbf{2}^-]}{[CO_3^{2-}]}}{1 + K_1\dfrac{[\mathbf{2}^-]}{[CO_3^{2-}]} + K_1K_2\dfrac{[\mathbf{2}^-]^2}{[CO_3^{2-}]^2} + K_1K_2K_3\dfrac{[\mathbf{2}^-]^3}{[CO_3^{2-}]^3}} \times \left(1 + 2K_2\frac{[\mathbf{2}^-]}{[CO_3^{2-}]} + 3K_2K_3\frac{[\mathbf{2}^-]^2}{[CO_3^{2-}]^2}\right) \tag{16}$$

obtained from the titration curve. Initial values of K_2 were obtained so as to give a best fit to the titration curve. Then, the iteration continued until the values of K_1, K_2, and K_3 giving the "best fit" titration curve were obtained.

Registry No. **1**, 89438-89-1; **2**, 147-84-2; $UO_2(CO_3)_3^{4-}$, 24646-13-7.

(19) As shown in Figure 3, the "total" absorbance of uranyl diethyldithiocarbamate complex increased in proportion to $[\mathbf{2}^-]$ till the $[\mathbf{2}^-]/[UO_2^{2+}]$ ratio reached the established stoichiometry[12] of 3. The observation clearly indicates not only that equilibrium proceeds successively U → **2**·U → $\mathbf{2}_2$U → $\mathbf{2}_3$U (see text) but also that all the absorption coefficients of the dithiocarbamate chromophore of **2**·UO_2, $\mathbf{2}_2UO_2$, and $\mathbf{2}_3UO_2$ at 450 nm are equal. In other words, the assumption that ϵ_2 equaled $2\epsilon_1$ and ϵ_3 equaled $3\epsilon_1$ must be satisfied.

Contribution from the Chemical Research Institute of Non-aqueous Solutions, Tohoku University, Katahira, Sendai, Japan 980

Correlation between the Hyperfine Coupling Constants of Donor Nitrogens and the Structures of the First Coordination Sphere in Copper Complexes As Studied by ^{14}N ENDOR Spectroscopy

Masamoto Iwaizumi,* Takanori Kudo, and Shouichi Kita[1]

Received April 8, 1985

Hyperfine (hf) coupling constants of coordinating nitrogens in copper(II) complexes with a pseudoplanar coordination array were collected with the help of ^{14}N ENDOR spectroscopy. The hf coupling constants are well grouped by the donor sets, N_4, *cis*-N_2O_2, *trans*-N_2O_2, and NO_3, as well as by the hybridized state of the nitrogens. Ligation at the axial position or distortion of the coordination array from planar to tetrahedral leads to decrease of the hf coupling constants. These correlations with the coordination structures indicate that the hf coupling constants of donor atoms may be useful to infer donor atoms and their configuration in the first coordination sphere for complexes with unknown metal binding sites, in conjunction with ESR or other studies.

Electron–nuclear double resonance (ENDOR) has been successfully used for resolving ligand hyperfine (hf) couplings buried in the ESR line widths in metal complexes.[2] In some cases, ligand hf interactions have been useful for obtaining information of structural details or for estimation or confirmation of metal binding sites. In the present work, we collected hf coupling constants of donor nitrogens in copper(II) complexes by the use of ENDOR spectroscopy, with the aim of finding general trends of the hf coupling constants of donor nitrogens and to find any correlation with the coordination structure. The copper(II) complexes treated here are limited to those having basically pseudoplanar array and donor sets of N_4, *cis*-N_2O_2, *trans*-N_2O_2, and NO_3. Frozen solutions and powder samples of the copper complexes were used for the ENDOR measurements in this work. The collected ^{14}N hf coupling data are well related to the donor sets and the hybrid state of nitrogens.

Experimental Section

Copper(II) complexes treated in this paper are listed in Table I. These complexes were synthesized according to literature cited in the table except for a few cases where a minor modification was made. Synthesized complexes were identified by elemental analyses and, for some cases, by also using optical absorption spectroscopy. Measurements of ENDOR spectra were made by a Varian E1700 ENDOR spectrometer at 10–25 K. The temperatures were controlled by a helium gas flow type cryostat.

Results and Discussion

The ESR spectrum of [Cu(aema)] and its ENDOR spectra recorded by different magnetic field settings indicated in the ESR spectrum are shown in Figures 1 and 2 as an example. In Figure 2, ^{14}N ENDOR signals due to two nonequivalent nitrogens are observed. As will be discussed later, the nitrogen signals on the low-frequency side can be assigned to the amine nitrogens and

(1) Present address: Department of Chemistry, Faculty of Science, Hirosaki University, Bunkyo-cho, Hirosaki, Japan 036.
(2) Schweiger, A. *Struct. Bonding (Berlin)* **1982**, *51*, 1.

0020-1669/86/1325-1546$01.50/0